Current Medicinal Chemistry, 2021, *28*, 4283-4294

RESEARCH ARTICLE

A Novel Dicationic Boron Dipyrromethene-based Photosensitizer for Antimicrobial Photodynamic Therapy against Methicillin-Resistant *Staphylococcus aureus*

Priyanga Dharmaratne[1,#], Ligang Yu[2,#], Roy Chi-Hang Wong[2], Ben Chun-Lap Chan[3,4], Kit-Man Lau[3,4], Baiyan Wang[1], Clara Bik San Lau[3,4], Kwok-Pui Fung[1,3,4,5], Dennis Kee-Pui Ng[2,*] and Margaret Ip[6,7,*]

[1]*School of Biomedical Sciences, Faculty of Medicine, The Chinese University of Hong Kong, Shatin, N.T., Hong Kong;* [2]*Department of Chemistry, The Chinese University of Hong Kong, Shatin, N.T., Hong Kong;* [3]*Institute of Chinese Medicine, The Chinese University of Hong Kong, Shatin, N.T., Hong Kong;* [4]*State Key Laboratory of Research on Bioactivities and Clinical Applications of Medicinal Plants, The Chinese University of Hong Kong, Shatin, N.T., Hong Kong;* [5]*CUHK-Zhejiang University Joint Laboratory on Natural Products and Toxicology Research, The Chinese University of Hong Kong, Shatin, N.T., Hong Kong;* [6]*Department of Microbiology, Faculty of Medicine, The Chinese University of Hong Kong, Prince of Wales Hospital, Shatin, N.T., Hong Kong;* [7]*Shenzhen Research Institute, The Chinese University of Hong Kong, 518057 Shenzhen, China*

Abstract: ***Background*:** We report herein the synthesis of a novel dicationic boron dipyrromethene derivative (compound **3**) which is symmetrically substituted with two trimethylammonium styryl groups.

***Methods*:** The antibacterial photodynamic activity of compound **3** was determined against sixteen methicillin-resistant *Staphylococcus aureus* (MRSA) strains, including four ATCC type strains (ATCC 43300, ATCC BAA-42, ATCC BAA-43, and ATCC BAA-44), two mutant strains [AAC(6')-APH(2") and RN4220/pUL5054], and ten non-duplicate clinical strains of hospital- and community-associated MRSA. Upon light irradiation, the minimum bactericidal concentrations of compound **3** were in the range of 1.56-50 μM against all the sixteen MRSA strains. Interestingly, compound **3** was not only more active than an analogue in which the ammonium groups are not directly connected to the n-conjugated system (compound **4**), but also showed significantly higher ($p < 0.05$) antibacterial potency than the clinically approved photosensitizer methylene blue. The skin irritation of compound **3** during topical application was tested on human 3-D skin constructs and proven to be non-irritant *in vivo* at concentrations below 1.250 mM. In the murine MRSA infected wound study, the colony forming unit reduction of compound **3** + PDT group showed significantly ($p < 0.05$) higher value (>2.5 $\log_{10}$) compared to other test groups except for the positive control.

***Conclusion*:** In conclusion, the present study provides a scientific basis for future development of compound **3** as a potent photosensitizer for photodynamic therapy for MRSA wound infection.

ARTICLE HISTORY

Received: July 13, 2020
Revised: October 14, 2020
Accepted: October 14, 2020

DOI:
10.2174/0929867328666201208095105

Keywords: Methicillin resistant *Staphylococcus aureus*, antimicrobial photodynamic therapy, boron dipyrromethene, murine wound infection model, photosensitizer, antibacterial potency.

*Address correspondence to these authors at the Department of Chemistry, The Chinese University of Hong Kong, Shatin, New Territories, Hong Kong; Tel: +852 39436375; Fax: +852 26035057; E-mail: dkpn@cuhk.edu.hk and Department of Microbiology, Faculty of Medicine, The Chinese University of Hong Kong, Prince of Wales Hospital, Shatin, New Territories, Hong Kong; Shenzhen Research Institute, The Chinese University of Hong Kong, 518057 Shenzhen, China; Tel: +852 35051265; Fax: +852 26473227; E-mail: margaretip@cuhk.edu.hk

[#]*These authors contributed equally to this work.*

1875-533X/21

1. INTRODUCTION

Photodynamic therapy (PDT) could be used to treat site-confined diseases *via* administration of a non-toxic photosensitizer (PS), followed by light irradiation of the site with an appropriate wavelength, usually in the visible region in the presence of molecular oxygen [1]. Combination of PS, light and molecular oxygen can generate highly reactive oxygen species (ROS) such as singlet oxygen ($^1O_2$), leading to non-selective cell destruction [1, 2]. PDT is proven as a successful treatment modality for many cell proliferative diseases such as localized solid tumours. It is particularly effective in treating skin cancers and other premalignant and non-malignant dermal abnormalities [2, 3]. Moreover, its application has been extended in treating cutaneous lesions caused by burns or wounds and for the disinfection of dental caries [2].

Besides the proven efficacy against eukaryotic cells [4], PDT is effective in killing pathogenic bacteria (prokaryotes). It is especially attractive because the technique has some unique advantages over conventional antibiotic treatments. For example, antibacterial PDT (aPDT) has an ability to inhibit both drug-resistant and drug-sensitive strains [5], and sometimes, it is even more potent against the former [6-8]. Furthermore, the absence of dark toxicity [9], fast antibacterial action [10], as well as no apparent drug resistance, are also its potential advantages [11, 12].

PSs commonly used in aPDT are organic molecules, with an extended π-bond conjugation that gives them a unique characteristic of harvesting long-wavelength visible light from electromagnetic radiation. Apart from the presence of an extended π-conjugated system, it is worth noting that the PSs suitable for aPDT usually require cationic moieties in their molecular structure to ascertain an effective interaction with the negatively charged bacterial cell wall, leading consequently to improved bacterial uptake of the PS [13]. Indeed, a range of cationic dyes such as cationic porphyrins (*e.g.* gallium(III) protoporphyrin IX [14] and 5,10,15,20-tetrakis(1-methylpyridinium-4-yl)porphyrin (**TMPyP**) [15]), polycationic phthalocyanines (*e.g.* zinc(II) phthalocyanine (ZnPc) **ZnPcE** [16], ZnPc with oligolysine chains [17] and tetracationic ZnPc chloride RLP068/Cl [18]) as well as some commercial dyes (*e.g.* methylene blue (MB) [19] and toluidine blue O [20]) were found to be able to eradicate different classes of bacteria.

Recently, a new class of PSs, the 4, 4-difluoro-4-bora-3a,4a-diaza-s-indacenes (known as boron dipyrromethene or simply the acronym BDP), have emerged to play a role in aPDT [21, 22]. These compounds, however, have some unfavourable features that may hinder their clinical applications. Owing to their high lipophilicity, aggregates may form in aqueous solutions. Besides, the λ_{max} of the π-π transition of these compounds appears at ca. 500 nm and the strong fluorescence does not favour the singlet oxygen formation. Therefore, structure modification should be warranted to circumvent the adverse effects of BDPs, making them effective for aPDT [13].

We report herein the synthesis of a novel dicationic and diiodinated BDP (compound **3**) which has good solubility in DMSO/aqueous solutions (<1:10 *v/v*), a high singlet oxygen quantum yield and a strong absorption at 600-700 nm. Although the aPDT activity of several BDPs against a few clinically relevant bacteria has been reported recently [21-24], the compatibility of BDPs in mammalian systems is poorly understood. As far as we know, the present study reported for the first time the photodynamic efficacy of cationic BDPs against a broad spectrum of clinically relevant methicillin-resistant *Staphylococcus aureus* (MRSA) strains. Following a systematic study on the *in vitro* efficacy of compound **3** using a previously reported structural analogue (compound **4**) for comparison, the highly potent compound **3** was thoroughly investigated in a murine MRSA wound infection model to determine the treatment efficacy *in vivo*. To our surprise, despite the structural and photophysical similarities of compound **3** and **4**, they possessed very different aPDT potencies. The difference in potency may be due to the different positively-charged functional groups. Although the effect of varying the number of positive charges on a photosensitizer has been reported [25], the effect of different kinds of positively-charged functional groups has not been studied in detail. The difference in potency between trialkylanilinum and tetraalkylammonium BDPs could also give clues in choosing the most effective charged functional groups when designing potent PSs. Further, we used the human three-dimensional skin constructs EpiDerm™ to predict the *in vivo* skin irritation of compound **3**. Overall, we provide a comprehensive experimental evidence on compound **3** as a promising BDP derivative against MRSA *in vitro* and *in vivo*.

2. MATERIALS AND METHODS

2.1. General

All the reactions were performed under a nitrogen atmosphere. *N*,*N*-dimethylformamide (DMF) was purified with an INERT solvent purification system (P-S-MD-5, Amesbury, MA, USA). All other solvents

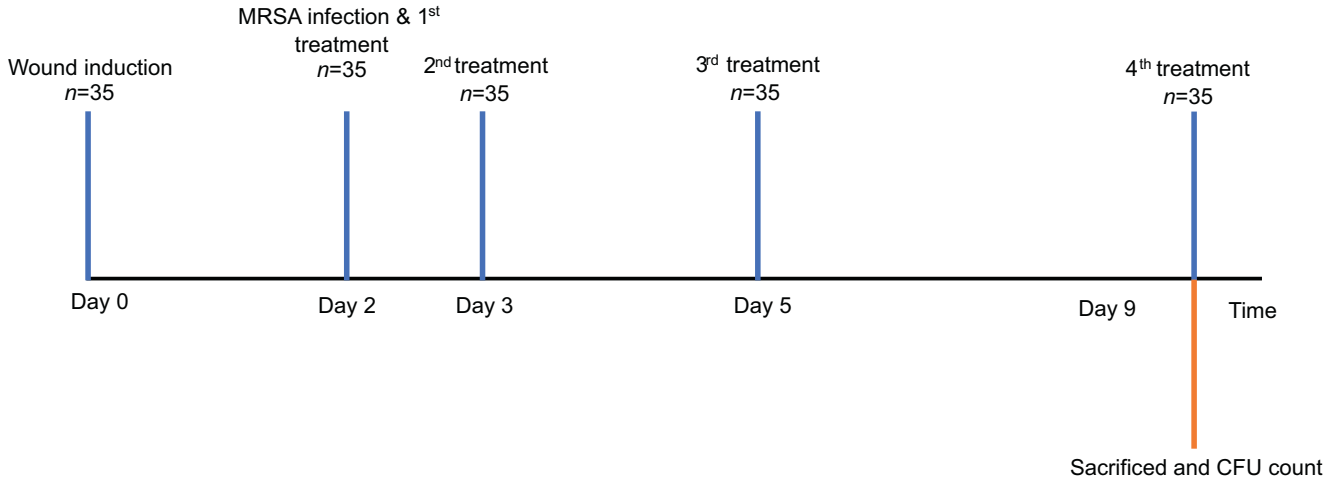

Fig. (1). Timeline for *in vivo* aPDT study. Four treatment cycles were performed at Day 2, 3, 5 and 9. After the 4th treatment, the mice were sacrificed for the CFU count.

and reagents were of the reagent grade and used as received. The course of reactions was monitored by thin layer chromatography (TLC) with Merck pre-coated silica gel 60 F254 plates (Merck Millipore, Darmstadt, Germany). Chromatographic purification was performed on silica gel (Macherey-Nagel, Düren, Germany; 230–400 mesh) with the indicated eluents. Compound **1** was prepared as described [37].

^{1}H and ^{13}C{^{1}H} NMR spectra were recorded on a Bruker AVANCE III 400 spectrometer (Billerica, MA, USA) (^{1}H, 400 MHz; ^{13}C, 100.6 MHz) in $CDCl_3$ or DMSO-d_6. Spectra were referenced internally by using the residual solvent [^{1}H, δ = 7.26 (for $CDCl_3$), δ = 2.50 (for DMSO-d_6)] or solvent [^{13}C, δ = 77.2 (for $CDCl_3$), δ = 39.5 (for DMSO-d_6)] resonances relative to $SiMe_4$. Electrospray ionization (ESI) mass spectra were recorded on a Thermo QEF MS mass spectrometer (Waltham, MA, USA). Electronic absorption and steady-state fluorescence spectra were taken on a Shimazu UV-1800 UV-Vis spectrophotometer (Tokyo, Tokyo Prefecture, Japan) and a Horiba FluoroMax spectrofluorometer (Kyoto, Kyoto Prefecture, Japan), respectively.

The bacterial strains, MRSA (ATCC 43300, ATCC BAA-42, ATCC BAA-43, ATCC BAA-44) and two mutant SA strains, AAC(6')-APH(2") and RN4220/pUL5054, were included for testing. The AAC(6')-APH(2") strain expresses the bi-functional enzyme AAC(6')-APH(2"), which is an aminoglycoside-modifying enzyme with the minimum inhibitory concentration (MIC): >128 μg/mL for gentamicin. The RN4220/pUL5054 strain shows a high level of erythromycin (MIC: 128 μg/mL) resistance due to the over-expression of *msr*(A) gene encoding for an ATP-binding cassette (ABC) transporter [27]. Five each from (non-duplicate) hospital (HA)- and community-associated (CA)-MRSAs were also included. These ten strains (clonal types ST239, ST30 and ST59) were specifically chosen due to their high prevalence rates in Hong Kong and neighbouring countries [28-30]. MRSAs were cultured in Mueller-Hinton Broth (MHB) for 18h at 37°C under an aerobic condition. The overnight culture was adjusted to 0.5 McFarland turbidity and diluted until the final concentration was 1.0×10^{6} CFU/mL. Altogether, 16 MRSAs were included for *in vitro* aPDT studies.

2.2. Synthesis

2.2.1. Synthesis of Compound 2

A mixture of compound **1** (100 mg, 135 μmol), 4-(dimethylamino)benzaldehyde (60.6 mg, 406 μmol), acetic acid (0.3 mL), piperidine (0.4 mL), and a catalytic amount of $Mg(ClO_4)_2$ in toluene (50 mL) was stirred under reflux with a Dean-Stark trap for 2 h, and then concentrated. The residue was purified by column chromatography to give compound **2** (52 mg, 38%) as a dark green solid. ^{1}H NMR (400 MHz, $CDCl_3$) δ 8.16 (d, J = 16.4 Hz, 2 H, C=CH), 7.53-7.58 (m, 6 H, ArH and C=CH), 7.15 (d, J = 8.4 Hz, 2 H, ArH), 7.04 (d, J = 8.8 Hz, 4 H, ArH), 6.74 (d, J = 8.8 Hz, 2H, ArH), 4.21 (t, J = 4.4 Hz, 2 H, CH_2), 3.93 (t, J = 4.8 Hz, 2 H, CH_2), 3.78-3.80 (m, 2 H, CH_2), 3.71-3.74 (m, 2 H, CH_2), 3.68-3.70 (m, 2 H, CH_2), 3.57-3.59 (m, 2 H, CH_2), 3.40 (s, 3 H, CH_3), 3.04 (s, 12 H, NCH_3), 1.48 (s,

6 H, CH_3). $^{13}C\{^1H\}$ NMR ($CDCl_3$) δ 17.7, 40.3, 59.1, 67.6, 69.7, 70.6, 70.7, 70.9, 72.0, 111.0, 112.1, 114.5, 115.3, 125.2, 127.9, 129.3, 129.9, 133.1, 136.5, 139.5, 144.8, 150.2, 151.2, 159.6 (Section **1** Supporting information, Fig. **S1**). HRMS (ESI) Calcd. for $C_{44}H_{49}BF_2I_2N_4O_4$ $[M]^+$ 1000.1906, found 1000.1898.

2.2.2. Synthesis of Compound 3

A mixture of compound **2** (25 mg, 25 μmol) and an excess amount of CH_3I (709 mg, 2.5 mmol) in DMF (10 mL) was stirred at 45-50 °C for 24 h. The mixture was then poured into excess ether to induce precipitation. The precipitate formed was collected by filtration and washed by ether to give compound **3** (24 mg, 95%) as a green solid. ^1H NMR (400 MHz, DMSO-d_6) δ 8.02-8.09 (m, 6 H, ArH and C=CH), 7.87 (d, J = 9.2 Hz, 4 H, ArH), 7.56 (d, J = 16.4 Hz, 2 H, C=CH), 7.35 (d, J = 8.4 Hz, 2 H, ArH), 7.18 (d, J = 8.4 Hz, 2 H, ArH), 4.19 (pseudo s, 2 H, CH_2), 3.80 (pseudo s, 2 H, CH_2), 3.66 (s, 18 H, NCH_3), 3.60-3.63 (m, 2 H, CH_2), 3.52-3.57 (m, 4 H, CH_2), 3.43-3.45 (m, 2 H, CH_2), 3.25 (s, 3 H, CH_3), 1.49 (s, 6 H, CH_3). $^{13}C\{^1H\}$ NMR (DMSO-d_6) δ 17.4, 30.8, 34.4, 35.8, 56.5, 58.1, 67.4, 68.9, 69.6, 69.8, 70.0, 71.3, 85.7, 115.6, 120.8, 121.5, 125.8, 128.4, 129.5, 133.5, 136.8, 137.5, 141.8, 146.5, 147.4, 149.8, 159.7, 162.3 (Section **1** Supporting information, Fig. **S2**). HRMS (ESI) Calcd. for $C_{46}H_{55}BF_2I_2N_4O_4$ $[M]^{2+}$ 515.1185, found 515.1181.

2.3. Determination of Fluorescence Quantum Yield (Φ_F)

The values of Φ_F were determined by the equation $\Phi_F(s) = (F_s/F_{ref})(A_{ref}/A_s)(n_s^2/n_{ref}^2)\ \Phi_F(ref)$, where subscript s refers to the sample solution while ref stands for the reference. F, A, and n are the measured fluorescence (area under the emission peak), the absorbance at the excitation position (610 nm), and the refractive index of the solvent, respectively [25]. Unsubstituted ZnPc in DMF was used as the reference (Φ_F = 0.28).

2.4. Determination of Singlet Oxygen Quantum Yield (Φ_Δ)

A solution of 1,3-diphenylisobenzofuran (DPBF, 30 μM) and different BDPs (1 μM) in DMF was illuminated with light from a 100 W halogen lamp under a colour filter with a cut-on wavelength at 610 nm (65CGA-610, Newport, Franklin, MA, 176 USA) upon passing through a water tank for cooling. The absorption maximum of DPBF at 415 nm was monitored along with the irradiation time. The values of Φ_Δ of the samples were determined by the equation $\Phi_\Delta(sample) = (W_{sample}/W_{ref})(I_{ref}/I_{sample})\Phi_\Delta(ref)$, where W and I are the DPBF photobleaching rate and the rate of light absorption, respectively [26]. Unsubstituted ZnPc in DMF was used as the reference (Φ_Δ = 0.56).

2.5. Assessment of *in vitro* PD-MBC

Minimum bactericidal concentrations (MBCs) of compounds **3**, **4**, and methylene blue (MB) were determined according to the method described previously [31]. Sample of each bacterial suspensions (100 μL) underwent a pre-irradiation step for 120 min with 100 μL of compounds **3** and **4** [Tween 80 and dimethyl sulfoxide (DMSO) concentrations were maintained ≤ 0.1% and 1% (*v*/*v*), respectively] in dark. Thereafter, the selected plates were illuminated with light intensity at 40 mW/cm^2 using a 300 W quartz-halogen lamp attenuated by a 5 cm layer of water (heat buffer) and a color glass filter with a cut-on wavelength of 610 nm (65CGA-610, Newport, Franklin, MA, 176 USA), as shown in Section **2** in Supporting information, Fig. **S3**. The illumination was carried out for 20 min, corresponding to a fluence (λ > 610 nm) of 48 J/cm^2 for PDT [16, 17, 31]. The dark toxicity of compounds **3** and **4** was evaluated by incubating the PSs along with the bacteria in dark. The effect of PDT alone was verified by replacing PSs with PBS and illuminating it for 20 min (48 J/cm^2).

The negative control did not receive any PSs nor light. Solvent toxicity (blank control) was also evaluated with 0.1% Tween 80 and 1% DMSO (*v*/*v*) to mimic the *in vitro* aPDT assay. MB was used as the positive control group, following the same protocol as that for the test (compounds **3** and **4**) groups. After an overnight incubation of the treated plates in dark, the MBC was determined using the method described previously [31].

2.6. *In vitro* EpiDerm™ Skin Irritation Test (EPI-200-SIT)

Reconstructed human three-dimensional skin constructs EpiDerm™ (EPI-200, MatTek Cor, Ashland, MA) were used for the toxicity test. The chemical exposure (compound **3** and **4**) followed by the tissue viability assay was executed exactly according to the manufacturer's instruction manual; the detailed method has been given in our previous publication [32].

2.7. Murine MRSA-infected Wound Model

The induction of MRSA infected murine skin wound model, PDT and enumeration of the CFU load was carried out according to the exact procedure de-

scribed in our previous report [32]. All animal experiments conformed to the university guidelines and approved by the Animal Experimentation Ethics Committee (Ref. no.16/176/MIS-5) of The Chinese University of Hong Kong. 4-6 weeks old male BALB/c mice (17-21 g) were supplied by Laboratory Animal Services Centre (LASEC), The Chinese University of Hong Kong. On Day 0, mice were anaesthetized intraperitoneally (i.p.) by ketamine (40 mg/kg) and xylazine (8 mg/kg), with the hair of the back shaved, and the skin cleansed with 10% povidone-iodine solution. A 4-5 mm diameter, full-thickness skin punch wound was established on subcutaneous tissue of the back of each mice. Buprenorphine, commercially available as Temgesic®, was administered (0.05 mg/kg) subcutaneously to the mice twice in the first 24 hours after wound induction to relieve pain.

Table 1. Conditions of the five groups of mice in the murine MRSA wound infection model.

Group	No. of Animals (*n*)	Treatment
A. Negative control group (NC)	7	50 μL of distilled water alone
B. Positive control group (PC)	7	50 μL of Fucidin® cream (containing fusidic acid 20 mg/g) alone
C. Light control group (LC)	7	50 μL of distilled water + PDT
D. Dark control group (DC)	7	50 μL of Compound **3** (1250 μM) alone
E. Test group (T)	7	50 μL of Compound **3** (1250 μM) + PDT

On Day 2, mice were re-anaesthetized and 20 μL aliquots of 1 x 10^8 CFU/mL suspension of MRSA RN4220/pUL5054 in MHB were spread evenly over the wound area using a micropipette. A dressing (Tegaderm™ film, 3M, USA) was applied to cover the wound immediately. The mice with infected wound were randomly divided into 5 cohorts (*n*=7 per each group), as listed in Table **1**.

First treatment was carried out 30 min after MRSA inoculation on Day 2. A 50 μL of 1250 μM compound **3** solution (to represent 100 x times of MBC value against MRSA RN4220/pUL5054 during *in vitro* studies), Fucidin® cream or distilled water was injected under the dressing (Tegaderm™) by syringe and allowed to spread over the wound.

For the Groups **C** and **E**, irradiation (Biolitec group, Bonn, Germany) was initiated immediately after compound inoculation with a single dosage of the laser at 1 W for 60 s, corresponding to 60 J/wound. After each treatment, the mice returned to individual ventilated cages (IVC) and Groups **D** and **E** were placed in the dark. The subsequent treatments were carried out on Day 3, Day 5 and Day 9, respectively, to cover 4 similar treatment cycles (Fig. **1**).

On Day 9, the mice were sacrificed by the administration of an intravenous dose of pentobarbital solution (Dorminal) after the last treatment (4th treatment). The wound (5 x 10 mm) was aseptically excised and the skin sample was homogenized in PBS (0.5 mL) for bacterial viability counts. Quantification of viable bacteria was performed by culturing serial dilutions (10 μL) of the homogenized suspension on blood agar plates and incubated at 37 °C for 24 h, and the CFU enumerated.

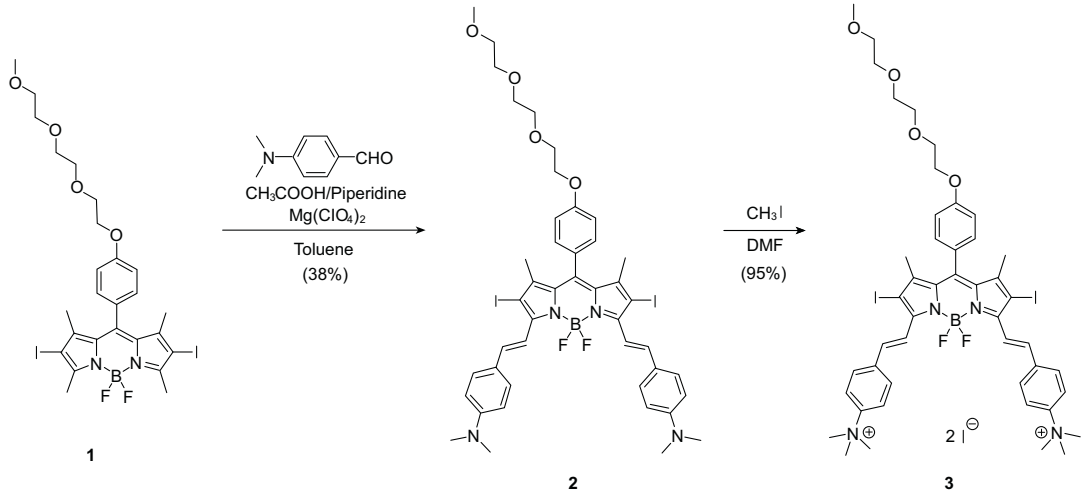

Fig. (2). Synthetic scheme of Compound 3.

3. RESULTS AND DISCUSSION

3.1. Design and Synthesis

The synthetic scheme used to prepare compound **3** is given in Fig. (**2**). The dicationic diiodinated BDP was synthesized using a triethylene glycol-conjugated diiodinated BDP (compound **1**) as a starting material. It underwent Knoevenagel condensation with 4-(dimethylamino)benzaldehyde in the presence of a catalytic amount of magnesium perchlorate to form the distyryl BDP **2**. It was then methylated with methyl iodide in DMF to yield the dicationic compound **3**. Both compounds **2** and **3** were purified readily by column chromatography and were characterized by various spectroscopic methods. Compound **3** was an analogue of the previously reported dicationic compound **4** (Fig. **3**) [31]. Both BDPs consist of two cationic moieties at the distyryl positions while the cationic groups in compound **4** are not directly connected to the π-conjugated system as in compound **3**.

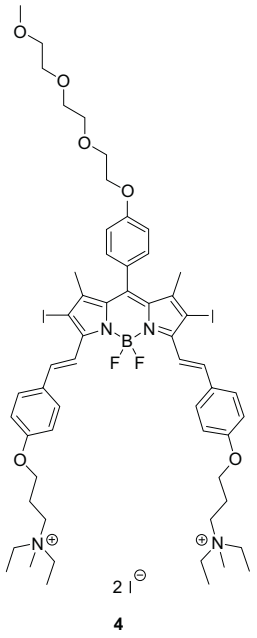

4

Fig. (3). Structure of Compound 4.

The electronic absorption and photophysical data of compound **3** were recorded in DMF and compared with that of compound **4**. The data are summarized in (Table **2**). The Q-band absorption was 31 nm blue-shifted for compound **3** when compared with that for compound **4** due to the difference in electronic effect between the trimethylammonium and alkoxyl substituents at the styryl positions in compound **3** and **4**, respectively. The fluorescence emission of compound **3** also appeared at a shorter wavelength (by 42 nm) than that of compound **4,** with a lower fluorescence quantum yield (0.14 versus 0.21 for compound **4**). Despite the difference in electronic absorption and fluorescence properties, the singlet oxygen generation efficiencies, as determined by the rate of decay of the singlet oxygen quencher DPBF and sensitized by the two BDPs in DMF, were very similar (0.52 and 0.54 for compounds **3** and **4**, respectively). The results suggested that the diiodo distyryl BDP core of the two compounds possessed a similar intrinsic photosensitizing ability.

3.2. *In vitro* photodynamic minimal bactericidal concentration (PD-MBC) studies

In (Table **2**), the MBCs of compounds **3** and **4** against a panel of reference strains are presented. The aPDT of compound **3** against MRSAs showed bactericidal activities at concentrations ranging from 1.56 to 50 μM (Table **3**). In contrast, compound **3** exhibited only a mild bactericidal activity in the absence of light (MBC = 100 to >100 μM) (Table **3**). The PDT effect thus increased the potency of compound **3** against clinically relevant MRSAs by 2 to > 64 times of magnitude when compared with its bactericidal activity in the dark (Table **3**).

The aPDT of compound **3** was compared with another PS (compound **4**) with similar structural moieties and λ_{max} value under identical conditions. The MBC values for compound **4** were >100 μM, indicating its significantly lower ($p < 0.05$) aPDT activity against

Table 2. Electronic absorption and photophysical data for compounds 3 and 4 in DMF.

Compound	λ_{max} /nm (log ε)	λ_{em} /nm[a]	Φ_F[a,b]	Φ_Δ[c,d]
3	349 (4.63), 425 (3.93), 630 (4.72)	648	0.14	0.52
4	316 (4.28), 379 (4.40), 446 (4.03), 661 (4.60)	690	0.21	0.54

[a]Excited at λ = 610 nm. [b]Relative to unsubstituted ZnPc (Φ_F = 0.28). [c]Excited at λ > 610 nm; [d]Relative to unsubstituted ZnPc (Φ_Δ = 0.56).

Table 3. The PD-MBC values for compounds 3, 4, and MB against 16 MRSA strains.

MRSA Type	MRSA Strain	Compound 3			Compound 4		MB		
		PDT (μM)	No PDT (μM)	aPDT potency[a]	PDT (μM)	No PDT (μM)	PDT (μM)	No PDT (μM)	aPDT potency
ATCC	43300	12.5	100[b] - > 100	8 - >8	>100	>100	625	>2500[c]	>4
ATCC	BAA 42	12.5 - 25	> 100	4 - 8	>100	>100	625	>2500	>4
ATCC	BAA 43	25-50	> 100	2 - >4	>100	>100	312.5-625	>2500	4->8
ATCC	BAA 44	12.5 - 25	100	4 - 8	>100	>100	312.5-625	>2500	4->8
Mutant	AAC(6')-APH(2'')	6.25	100	16	>100	>100	625-1250	>2500	2->4
Mutant	RN4220 /pUL5054	12.5 - 25	100 - > 100	4 - >8	>100	>100	1250-2500	>2500	2->4
CA[d]	W44	6.25 - 12.5	100 - > 100	8 - >16	>100	>100	2500	>2500	>1
CA	W45	12.5 - 50	> 100	2 - >8	>100	>100	1250-2500	>2500	1->2
CA	W46	25 - 50	> 100	2 - >4	>100	>100	2500	>2500	>1
CA	W47	3.125 - 6.25	> 100	16 - >32	>100	>100	2500	>2500	>1
CA	W48	3.125 - 12.5	> 100	8 - >32	>100	>100	2500	>2500	>1
HA[e]	W231	1.56 - 6.25	> 100	16 - >64	>100	>100	2500	>2500	>1
HA	W232	3.125 - 6.25	> 100	16 - >32	>100	>100	2500	>2500	>1
HA	W233	6.25	> 100	> 16	>100	>100	2500	>2500	>1
HA	W234	12.5	> 100	>8	>100	>100	2500	>2500	>1
HA	W235	1.56 - 3.125	> 100	32 - >64	>100	>100	2500	>2500	>1

[a]Fold reduction in compound 3, 4 and MB concentration, relative to dark toxicity (no light exposure); [b]Highest concentration tested for compound 3 and 4; [c]Highest concentration tested for MB; [d]Community-associated; [e]Hospital-associated.

MRSAs when compared with compound **3**. The aPDT of MB was also tested and included as a control for comparison. It is a mono-cationic phenothiazine that has long been studied and already in clinical use. *In vitro* aPDT studies using a $\lambda > 610$ nm filter cut-on light revealed that MB possessed aPDT activity at significantly ($p < 0.05$) higher concentrations than compound **3**.

These results were unexpected because the structural and photophysical characteristics of compounds **3** and **4** were similar. The similar singlet oxygen quantum yields of compounds **3** and **4** suggested that the difference in potency should not be inflicted by the intrinsic efficiency of the PSs to produce ROS. Instead, the triakylanilium and tetraakylammonium groups responsible for the cationic charges in compounds **3** and **4**, respectively, may vary in their extent of bacterial uptake. While most of the aPDT studies focused on the effect of the number of cationic charges on the PSs, the present result suggested that simply incorporating sufficient cationic groups does not translate the design of potent antimicrobial PSs. To the best of our knowledge, only Alves *et al*. reported the effect of the position of cationic charges in photoinactivation, where the symmetry of the cationic groups has a significant impact on the antibacterial potency [33]. Since their finding could not exactly explain the effect difference observed in this paper, further study on these charge-bearing amine groups needs to be done to clarify their contribution in the antibacterial potency, whether it is from the position of the charges, the flexibility of the charges, or the specific type of cationic charges.

The *in vitro* studies (Table **3**) showed that compound **4** has (> 100 μM) significantly ($p < 0.05$) higher MBC values than compound **3** against the whole panel of bacteria. Therefore, we have refrained from further investigation of compound **4** on human 3-D skin constructs to determine cytotoxicity on *in vivo* MRSA infected wound model in mice due to their intrinsic toxicity at very high concentrations.

3.3. *In vitro* EpiDerm™ Skin Irritation Test

The toxicity of compound **3** was determined by a skin irritation test as applied on human 3-D skin constructs (EpiDerm™). As shown in (Fig. **4**), the cell viability of EPI-200 cells was >50% at 1250 μM (100 x times of MBC value against MRSA RN4220 /pUL5054). This indicates that compound **3** did not manifest toxicity (according to the EU and GHS classi-

fication) on human 3-D skin constructs EpiDerm™, at ≤1250 μM concentration (Section **3** supporting information). This finding supports the safe use of compound **3** topically for aPDT.

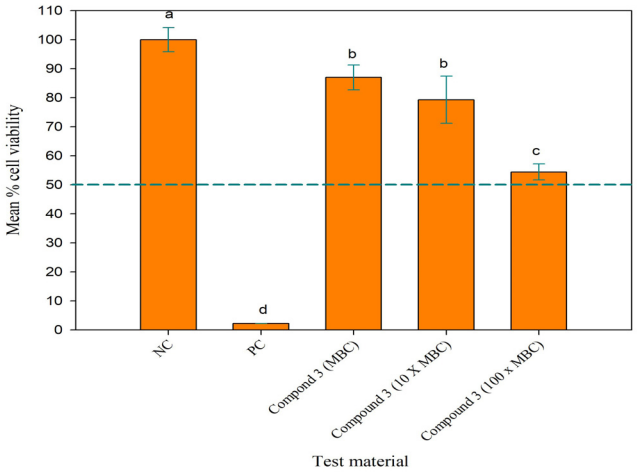

Fig. (4). Cell viability of EPI-200 cells under different treatments. They were treated with DPBS [Negative control (NC)], 5% SDS [Positive control (PC)], 12.5 μM of Compound 3 [equivalent to MBC against MRSA RN 4220/pUL5054 (Compound 3 (MBC)], 125 μM of Compound 3 [equivalent to 10 x MBC against MRSA RN 4220/pUL5054 (Compound 3 (10 x MBC)] or 1250 μM of Compound 3 [equivalent to 100 x MBC against MRSA RN 4220/pUL5054 (Compound 3 (100 x MBC)]. Experimental data are expressed as mean ± SD (n=3). Means that do not share a letter are significantly different. Mean cell viability > 50% for the Compound 3 (MBC, 10 x MBC or 100 x MBC) implies that Compound 3 did not pose any skin irritation on human 3-D skin construct at concentrations below 1250 μM. (*A higher resolution / colour version of this figure is available in the electronic copy of the article*).

3.4. Murine MRSA Wound Infection Model (*in vivo* aPDT)

Compounds **3** (1250 μM) were directly applied topically to the infection wounds for each treatment and NIR (λ > 610 nm) was applied in 4 doses over 9 days with 60 J/wound. The bacterial load at Day 9 is given in Fig. (**5**). PDT alone (Group **C**) shows just 0.67 ± 0.21 $\log_{10}$ CFU reduction Fig. (**5**), indicating that the effect of PDT alone does not have a direct impact on the reduction of bacterial load. We compared the wound appearances before and after the PDT cycles and noticed there was no photothermal damage or skin irritation on or around the wounds (Supporting information, Section **4**, Fig. **S4**). For compound **3**, dark control group (Group **D**), showed a 0.75 ± 0.36 $\log_{10}$ CFU reduction Fig. (**5**) and the value is comparable with Group **C** (PDT alone). Irradiation of compound **3**-treated cohort (Group **E**) ascertained 2.85 ± 0.32 $\log_{10}$ CFU reduction and the value is significantly higher ($p < 0.05$) than all other treated groups, except for Group **B** (Positive control, Fucidin® cream) that attained complete eradication of bacteria Fig. (**5**). Here we used Fucidin® cream as a positive control instead of MB because it is currently used topically in the clinical setting for the treatment of *S. aureus* skin and soft tissue infections. Hence, we wanted to compare the effect and activity of our PDT therapy (as an alternative approach) with the conventional treatment modality. A similar observation has been made by other investigators [34-37], where PDT-treated infected wounds had significantly ($P < 0.05$) lower bacterial counts at all time points than irradiation alone or PS alone-treated groups.

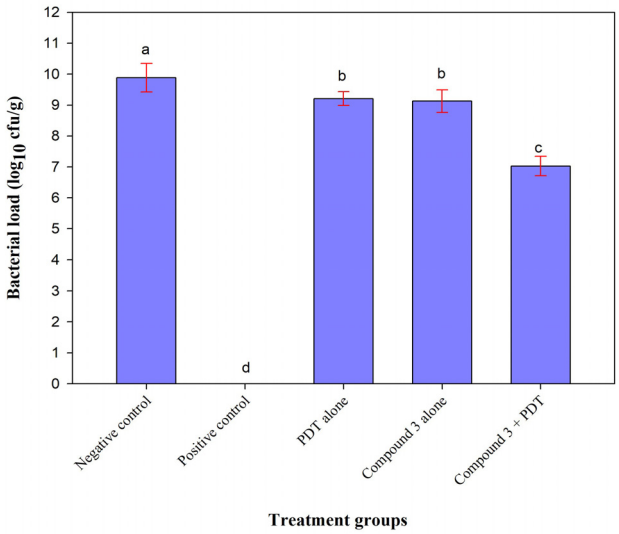

Fig. (5). *In vivo* aPDT efficiency against MRSA RN4220/pUL5054 infected wound mediated by 1250 μM concentration of Compound 3. Experimental data are expressed as mean ± SD (n=7). Means that do not share a letter are significantly different. Compound 3 + PDT cohort showed significantly lower ($p < 0.05$) bacterial load after 4 treatment cycles, compared to all other treated groups, except positive control (2% Fusidic cream). (*A higher resolution / colour version of this figure is available in the electronic copy of the article*).

In the animal study, we inoculated the bacteria to the wounds 2 days after wound induction. It mimicked the clinical situation of postoperative infection. Unlike many other *in vivo* aPDT studies [36-39], we identified that multiple treatment cycles (4 cycles) rather than a single high dosage of light were more effective in our

preliminary studies (data not shown). Furthermore, we found that continuous treatment was also inappropriate due to the possible photothermal effect. Therefore, we optimized the light treatment protocol so that more treatments were given early in the infection (Fig. **1**) in order to reduce the bacterial load, while minimizing delay in healing. The regimen of repeated treatment was supported by Lambrechts *et al*. [39] in their discussion as an improving step to decrease the bacterial load in *S. aureus*-infected burn wounds in mice.

DMSO is a polar aprotic solvent that enhances drug penetration through the skin and it is incorporated into an idoxuridine-based commercial preparation to treat herpetic infections of the skin [40]. Several studies [40-42] have used 10- 25% DMSO/PBS mixture to dissolve PS and observed a light dose-dependent bacterial load reduction by increasing permeability towards deeper infected tissues. However, in the current investigation, <1% (*v/v*) DMSO was used and a higher percentage DMSO may be considered to improve its permeability towards deeper infected tissues and induce a subsequent increase in aPDT potency in full thick wound *in vivo*.

The post-treatment monitoring of infection sites was performed after the final treatment by measuring the wound size and change in body weight of animals. The size of wounds in the Negative Control Group (Group **A**) was slightly larger but there was no significant difference in wound size among all groups (data not shown).

Furthermore, there occurred a progressive body weight increase in all groups over the treatment period (9 days, Section **5** Supporting information, Fig. **S5**), suggesting that PDT did not have any observable side effects. Our observation was in line with that of Mai *et al*. [43], where they found that mice with untreated infected wounds exhibited progressive increases in body weight over the 5-day treatment cycle and mice with PDT-treated infected wounds exhibited a similar pattern, regardless of the concentration of the photosensitizer.

CONCLUSION

In summary, a novel symmetric dicationic boron dipyrromethene with increased hydrophilic properties was synthesized. The photophysical characteristics of this compound **3** and its structural analogue compound **4** were comparable, suggesting their similar intrinsic photosensitizing ability. However, compound **3** ascertained significantly higher ($p < 0.05$) *in vitro* aPDT efficacy against MRSA than its structural analogue (compound **4**), implying other factors such as the type of cationic charge (triakylanilium and tetraakylammonium) and their positions to also alter the activities. The encouraging results obtained using a dicationic compound **3** as an antimicrobial photosensitizer combined with NIR ($\lambda > 610$ nm) both *in vitro* and *in vivo* warrant further investigations on their mechanistic action, aPDT potency as a function of positive charge carrying group, and selectivity towards MRSA.

AUTHORS' CONTRIBUTIONS

Priyanga Dharmaratne: Completed *in vitro* aPDT studies, completed skin irritation test using EpiDerm™, helped to perform *in vivo* aPDT studies and drafted the manuscript.

Ligang Yu and Roy Chi-Hang Wong: Synthesized Compounds 3 and 4, evaluated the photophysical data and revised the manuscript.

Ben Chun-Lap Chan: Designed and performed *in vivo* aPDT studies, and revised the manuscript.

Kit-Man Lau: Designed and performed *in vivo* aPDT studies, and revised the manuscript.

Baiyan Wang: Revised the manuscript.

Clara Bik San Lau: Commented on the study and revised the manuscript.

Dennis Kee-Pui Ng: Advised on the synthesis of compounds 3 and 4 and provided critical feedback on the manuscript.

Dennis Kee-Pui Ng and Margaret Ip: Conceptualized, initiated, and oversaw the project and provided critical feedback on the manuscript.

LIST OF ABBREVIATIONS

aPDT	=	Antimicrobial Photodynamic Therapy
ATCC	=	American Type Culture Collection
BDP	=	Boron Dipyrromethene
CA	=	Community Associated
CFU	=	Colony Forming Unit
DMEM	=	Dulbecco's Minimum Essential Medium
DMF	=	Dimethylformamide
DMSO	=	Dimethyl Sulfoxide
DPBF	=	Diphenylisobenzofuran
ESBL	=	Extended Spectrum β-lactamase
HA	=	Hospital Associated
MB	=	Methylene Blue
MBC	=	Minimum Bactericidal Concentration

MDR = Multi-drug Resistant

MHB = Mueller Hinton Broth

MIC = Minimum Inhibitory Concentration

MRSA = Methicillin-resistant *Staphylococcus aureus*

MSSA = Methicillin-sensitive *Staphylococcus aureus*

NIR = Near Infrared

PS = Photosensitizer

PBS = Phosphate Buffer Saline

ROS = Reactive Oxygen Species

ST = Sequential Type

VRSA = Vancomycin-resistant *S. aureus*

ZnPc = Zn(II) phthlocyanines

TMPyP = 5,10,15,20-tetrakis(1-methylpyridinium-4-yl)-porphyrin.

ETHICS APPROVAL AND CONSENT TO PARTICIPATE

The study has been approved by the University Animal Experimentation Ethics Committee (AEEC; Reference no.:16-176-MIS) and conducted at the Laboratory Animal Services Centre at the Chinese University of Hong Kong.

HUMAN AND ANIMAL RIGHTS

The use of animals is in compliance with International Guiding Principles for Biomedical Research involving animals and The Hong Kong Code of Practice for care and use of animals for experimental purposes.

CONSENT FOR PUBLICATION

Not applicable

AVAILABILITY OF DATA AND MATERIALS

Not applicable.

FUNDING

This work has been partially supported by a grant from the Health and Medical Research Fund (HMRF 16151202), and by the Si Yuan Foundation, HKSAR, China.

CONFLICT OF INTEREST

The authors declare no conflict of interest, financial or otherwise.

ACKNOWLEDGEMENTS

Declared none.

SUPPLEMENTARY MATERIAL

Supplementary material is available on the publisher's web site along with the published article.

REFERENCES

[1] Moan, J. Properties for optimal PDT sensitizers. *J. Photochem. Photobiol. B,* **1990**, *5*(3-4), 521-524. http://dx.doi.org/10.1016/1011-1344(90)85064-4 PMID: 2115921

[2] Moan, J.; Peng, Q. An outline of the history of PDT. *Photody. Ther.,* **1993**, *2*, 1-18. http://dx.doi.org/10.1039/9781847551658-00001

[3] Dai, T.; Huang, Y.Y.; Hamblin, M.R. Photodynamic therapy for localized infections--state of the art. *Photodiagn. Photodyn. Ther.,* **2009**, *6*(3-4), 170-188. http://dx.doi.org/10.1016/j.pdpdt.2009.10.008 PMID: 19932449

[4] Agostinis, P.; Berg, K.; Cengel, K.A.; Foster, T.H.; Girotti, A.W.; Gollnick, S.O.; Hahn, S.M.; Hamblin, M.R.; Juzeniene, A.; Kessel, D.; Korbelik, M.; Moan, J.; Mroz, P.; Nowis, D.; Piette, J.; Wilson, B.C.; Golab, J. Photodynamic therapy of cancer: an update. *CA Cancer J. Clin.,* **2011**, *61*(4), 250-281. http://dx.doi.org/10.3322/caac.20114 PMID: 21617154

[5] Usacheva, M.N.; Teichert, M.C.; Biel, M.A. Comparison of the methylene blue and toluidine blue photobactericidal efficacy against gram-positive and gram-negative microorganisms. *Lasers Surg. Med.,* **2001**, *29*(2), 165-173. http://dx.doi.org/10.1002/lsm.1105 PMID: 11553906

[6] Wainwright, M.; Crossley, K.B. Methylene Blue--a therapeutic dye for all seasons? *J. Chemother.,* **2002**, *14*(5), 431-443. http://dx.doi.org/10.1179/joc.2002.14.5.431 PMID: 12462423

[7] Topaloglu, N.; Gulsoy, M.; Yuksel, S. Antimicrobial photodynamic therapy of resistant bacterial strains by indocyanine green and 809-nm diode laser. *Photomed. Laser Surg.,* **2013**, *31*(4), 155-162. http://dx.doi.org/10.1089/pho.2012.3430 PMID: 23402392

[8] Grinholc, M.; Szramka, B.; Kurlenda, J.; Graczyk, A.; Bielawski, K.P. Bactericidal effect of photodynamic inactivation against methicillin-resistant and methicillin-susceptible Staphylococcus aureus is strain-dependent. *J. Photochem. Photobiol. B,* **2008**, *90*(1), 57-63. http://dx.doi.org/10.1016/j.jphotobiol.2007.11.002 PMID: 18093839

[9] Liu, Y.; Qin, R.; Zaat, S.A.J.; Breukink, E.; Heger, M. Antibacterial photodynamic therapy: overview of a promising approach to fight antibiotic-resistant bacterial infections. *J. Clin. Transl. Res.,* **2015**, *1*(3), 140-167. http://dx.doi.org/10.18053/jctres.201503.002 PMID: 30873451

[10] Dai, T.; Tegos, G.P.; Zhiyentayev, T.; Mylonakis, E.; Hamblin, M.R. Photodynamic therapy for methicillin-resistant *Staphylococcus aureus* infection in a mouse skin abrasion model. *Lasers Surg. Med.,* **2010**, *42*(1), 38-44. http://dx.doi.org/10.1002/lsm.20887 PMID: 20077489

[11] Bartolomeu, M.; Rocha, S.; Cunha, Â.; Neves, M.G.; Faustino, M.A.; Almeida, A. Effect of photodynamic thera-

py on the virulence factors of *Staphylococcus aureus*. *Front. Microbiol.,* **2016**, *7*, 267. http://dx.doi.org/10.3389/fmicb.2016.00267 PMID: 27014198

[12] Lauro, F.M.; Pretto, P.; Covolo, L.; Jori, G.; Bertoloni, G. Photoinactivation of bacterial strains involved in periodontal diseases sensitized by porphycene-polylysine conjugates. *Photochem. Photobiol. Sci.,* **2002**, *1*(7), 468-470. http://dx.doi.org/10.1039/b200977c PMID: 12659156

[13] Caruso, E.; Banfi, S.; Barbieri, P.; Leva, B.; Orlandi, V.T. Synthesis and antibacterial activity of novel cationic BODIPY photosensitizers. *J. Photochem. Photobiol. B,* **2012**, *114*, 44-51. http://dx.doi.org/10.1016/j.jphotobiol.2012.05.007 PMID: 22682365

[14] Morales-de-Echegaray, A.V.; Maltais, T.R.; Lin, L.; Younis, W.; Kadasala, N.R.; Seleem, M.N.; Wei, A. Rapid uptake and photodynamic inactivation of staphylococci by Ga(III)-protoporphyrin IX. *ACS Infect. Dis.,* **2018**, *4*(11), 1564-1573. http://dx.doi.org/10.1021/acsinfecdis.8b00125 PMID: 30175917

[15] Maisch, T.; Spannberger, F.; Regensburger, J.; Felgenträger, A.; Bäumler, W. Fast and effective: intense pulse light photodynamic inactivation of bacteria. *J. Ind. Microbiol. Biotechnol.,* **2012**, *39*(7), 1013-1021. http://dx.doi.org/10.1007/s10295-012-1103-3 PMID: 22354734

[16] Ke, M.R.; Eastel, J.M.; Ngai, K.L.; Cheung, Y.Y.; Chan, P.K.; Hui, M.; Ng, D.K.P.; Lo, P.C. Photodynamic inactivation of bacteria and viruses using two monosubstituted zinc(II) phthalocyanines. *Eur. J. Med. Chem.,* **2014**, *84*, 278-283. http://dx.doi.org/10.1016/j.ejmech.2014.07.022 PMID: 25036788

[17] Ke, M.R.; Eastel, J.M.; Ngai, K.L.; Cheung, Y.Y.; Chan, P.K.; Hui, M.; Ng, D.K.P.; Lo, P.C. Oligolysine-conjugated zinc(II) phthalocyanines as efficient photosensitizers for antimicrobial photodynamic therapy. *Chem. Asian J.,* **2014**, *9*(7), 1868-1875. http://dx.doi.org/10.1002/asia.201402025 PMID: 24799418

[18] Simonetti, O.; Cirioni, O.; Orlando, F.; Alongi, C.; Lucarini, G.; Silvestri, C.; Zizzi, A.; Fantetti, L.; Roncucci, G.; Giacometti, A.; Offidani, A.; Provinciali, M. Effectiveness of antimicrobial photodynamic therapy with a single treatment of RLP068/Cl in an experimental model of *Staphylococcus aureus* wound infection. *Br. J. Dermatol.,* **2011**, *164*(5), 987-995. http://dx.doi.org/10.1111/j.1365-2133.2011.10232.x PMID: 21275941

[19] Street, C.N.; Pedigo, L.A.; Loebel, N.G. Energy dose parameters affect antimicrobial photodynamic therapy-mediated eradication of periopathogenic biofilm and planktonic cultures. *Photomed. Laser Surg.,* **2010**, *28*(Suppl. 1), S61-S66. http://dx.doi.org/10.1089/pho.2009.2622 PMID: 20666581

[20] Tang, H.M.; Hamblin, M.R.; Yow, C.M. A comparative *in vitro* photoinactivation study of clinical isolates of multidrug-resistant pathogens. *J. Infect. Chemother.,* **2007**, *13*(2), 87-91. http://dx.doi.org/10.1007/s10156-006-0501-8 PMID: 17458675

[21] Frimannsson, D.O.; Grossi, M.; Murtagh, J.; Paradisi, F.; O'Shea, D.F. Light induced antimicrobial properties of a brominated boron difluoride (BF(2)) chelated tetraarylazadipyrromethene photosensitizer. *J. Med. Chem.,* **2010**, *53*(20), 7337-7343. http://dx.doi.org/10.1021/jm100585j PMID: 20879783

[22] Carpenter, B.L.; Situ, X.; Scholle, F.; Bartelmess, J.; Weare, W.W.; Ghiladi, R.A. Antiviral, antifungal and antibacterial activities of a BODIPY-based photosensitizer. *Molecules,* **2015**, *20*(6), 10604-10621. http://dx.doi.org/10.3390/molecules200610604 PMID: 26060922

[23] Alnoman, R.B.; Parveen, S.; Hagar, M.; Ahmed, H.A.; Knight, J.G. A new chiral boron-dipyrromethene (BODIPY)-based fluorescent probe: molecular docking, DFT, antibacterial and antioxidant approaches. *J. Biomol. Struct. Dyn.,* **2019**, *2*, 1-14. http://dx.doi.org/10.1080/07391102.2019.1701555 PMID: 31809642

[24] Orlandi, V.T.; Rybtke, M.; Caruso, E.; Banfi, S.; Tolker-Nielsen, T.; Barbieri, P. Antimicrobial and anti-biofilm effect of a novel BODIPY photosensitizer against *Pseudomonas aeruginosa* PAO1. *Biofouling,* **2014**, *30*(8), 883-891. http://dx.doi.org/10.1080/08927014.2014.940921 PMID: 25184429

[25] Eaton, D.F. International union of pure and applied chemistry organic chemistry division commission on photochemistry. Reference materials for fluorescence measurement. *J. Photochem. Photobiol. B,* **1988**, *2*(4), 523-531. http://dx.doi.org/10.1016/1011-1344(88)85081-4 PMID: 3150004

[26] Maree, M.; Kuznetsova, N.; Nyokong, T. Silicon octaphenoxyphthalocyanines: photostability and singlet oxygen quantum yields. *J. Photochem. and Photobio.,* **2011**, *40*, 117-125. http://dx.doi.org/10.1016/S1010-6030(01)00409-9

[27] Ross, J.I.; Eady, E.A.; Cove, J.H.; Cunliffe, W.J.; Baumberg, S.; Wootton, J.C. Inducible erythromycin resistance in staphylococci is encoded by a member of the ATP-binding transport super-gene family. *Mol. Microbiol.,* **1990**, *4*(7), 1207-1214. http://dx.doi.org/10.1111/j.1365-2958.1990.tb00696.x PMID: 2233255

[28] Ip, M.; Yung, R.W.; Ng, T.K.; Luk, W.K.; Tse, C.; Hung, P.; Enright, M.; Lyon, D.J. Contemporary methicillin-resistant *Staphylococcus aureus* clones in Hong Kong. *J. Clin. Microbiol.,* **2005**, *43*(10), 5069-5073. http://dx.doi.org/10.1128/JCM.43.10.5069-5073.2005 PMID: 16207964

[29] Li, J.; Wang, L.; Ip, M.; Sun, M.; Sun, J.; Huang, G.; Wang, C.; Deng, L.; Zheng, Y.; Fu, Z.; Li, C.; Shang, Y.; Zhao, C.; Yu, S.; Yao, K.; Yang, Y.; Shen, X. Molecular and clinical characteristics of clonal complex 59 methicillin-resistant *Staphylococcus aureus* infections in Mainland China. *PLoS One,* **2013**, *8*(8), e70602. http://dx.doi.org/10.1371/journal.pone.0070602 PMID: 23950969

[30] Wong, J.W.; Ip, M.; Tang, A.; Wei, V.; Wong, S.; Riley, S.; Kwok, K.O. Prevalence and risk factors of community-associated methicillin-resistant *Staphylococcus aureus* (CA-MRSA) carriage in Asia-Pacific region from 2000 to 2016: a systematic review and meta-analysis. *Int. J. Infect. Dis.,* **2018**, *73*, 135-136. http://dx.doi.org/10.1016/j.ijid.2018.04.3722

[31] Dharmaratne, P.; Wong, R.C.H.; Wang, J.; Lo, P.C.; Wang, B.; Chan, B.C.L.; Lau, K.M.; Lau, C.B.S.; Fung,

K.P.; Ip, M.; Ng, D.K.P. Synthesis and *in vitro* photodynamic activity of cationic boron dipyrromethene-based photosensitizers against methicillin-resistant *Staphylococcus aureus*. *Biomedicines,* **2020**, *8*(6), 140-154. http://dx.doi.org/10.3390/biomedicines8060140 PMID: 32485946

[32] Dharmaratne, P.; Wang, B.; Wong, R.C.H.; Chan, B.C.L.; Lau, K.M.; Ke, M.R.; Lau, C.B.S.; Ng, D.K.P.; Fung, K.P.; Ip, M. Monosubstituted tricationic Zn(II) phthalocyanine enhances antimicrobial photodynamic inactivation (aPDI) of methicillin-resistant *Staphylococcus aureus* (MRSA) and cytotoxicity evaluation for topical applications: *in vitro* and *in vivo* study. *Emerg. Microbes Infect.,* **2020**, *9*(1), 1628-1637. http://dx.doi.org/10.1080/22221751.2020.1790305 PMID: 32619386

[33] Alves, E.; Costa, L.; Carvalho, C.M.; Tomé, J.P.; Faustino, M.A.; Neves, M.G.; Tomé, A.C.; Cavaleiro, J.A.; Cunha, A.; Almeida, A. Charge effect on the photoinactivation of Gram-negative and Gram-positive bacteria by cationic meso-substituted porphyrins. *BMC Microbiol.,* **2009**, *9*, 70. http://dx.doi.org/10.1186/1471-2180-9-70 PMID: 19368706

[34] Vecchio, D.; Dai, T.; Huang, L.; Fantetti, L.; Roncucci, G.; Hamblin, M.R. Antimicrobial photodynamic therapy with RLP068 kills methicillin-resistant *Staphylococcus aureus* and improves wound healing in a mouse model of infected skin abrasion PDT with RLP068/Cl in infected mouse skin abrasion. *J. Biophotonics,* **2013**, *6*(9), 733-742. http://dx.doi.org/10.1002/jbio.201200121 PMID: 22987338

[35] Demidova, T.N.; Gad, F.; Zahra, T.; Francis, K.P.; Hamblin, M.R. Monitoring photodynamic therapy of localized infections by bioluminescence imaging of genetically engineered bacteria. *J. Photochem. Photobiol. B,* **2005**, *81*(1), 15-25. http://dx.doi.org/10.1016/j.jphotobiol.2005.05.007 PMID: 16040251

[36] Hamblin, M.R.; Zahra, T.; Contag, C.H.; McManus, A.T.; Hasan, T. Optical monitoring and treatment of potentially lethal wound infections *in vivo*. *J. Infect. Dis.,* **2003**, *187*(11), 1717-1725. http://dx.doi.org/10.1086/375244 PMID: 12751029

[37] Hamblin, M.R.; O'Donnell, D.A.; Murthy, N.; Contag, C.H.; Hasan, T. Rapid control of wound infections by targeted photodynamic therapy monitored by *in vivo* bioluminescence imaging. *Photochem. Photobiol.,* **2002**, *75*(1), 51-57. http://dx.doi.org/10.1562/0031-8655(2002)075<0051:RCOWIB>2.0.CO;2 PMID: 11837327

[38] Busch, N.A.; Zanzot, E.M.; Loiselle, P.M.; Carter, E.A.; Allaire, J.E.; Yarmush, M.L.; Warren, H.S. A model of infected burn wounds using *Escherichia coli* O18:K1:H7 for the study of gram-negative bacteremia and sepsis. *Infect. Immun.,* **2000**, *68*(6), 3349-3351. http://dx.doi.org/10.1128/IAI.68.6.3349-3351.2000 PMID: 10816484

[39] Lambrechts, S.A.; Demidova, T.N.; Aalders, M.C.; Hasan, T.; Hamblin, M.R. Photodynamic therapy for *Staphylococcus aureus* infected burn wounds in mice. *Photochem. Photobiol. Sci.,* **2005**, *4*(7), 503-509. http://dx.doi.org/10.1039/b502125a PMID: 15986057

[40] Williams, A.C.; Barry, B.W. Penetration enhancers. *Adv. Drug Deliv. Rev.,* **2004**, *56*(5), 603-618. http://dx.doi.org/10.1016/j.addr.2003.10.025 PMID: 15019749

[41] Malik, Z.; Kostenich, G.; Roitman, L.; Ehrenberg, B.; Orenstein, A. Topical application of 5-aminolevulinic acid, DMSO and EDTA: protoporphyrin IX accumulation in skin and tumours of mice. *J. Photochem. Photobiol. B,* **1995**, *28*(3), 213-218. http://dx.doi.org/10.1016/1011-1344(95)07117-K PMID: 7623186

[42] De Rosa, F.S.; Marchetti, J.M.; Thomazini, J.A.; Tedesco, A.C.; Bentley, M.V. A vehicle for photodynamic therapy of skin cancer: Influence of dimethylsulphoxide on 5-aminolevulinic acid *in vitro* cutaneous permeation and *in vivo* protoporphyrin IX accumulation determined by confocal microscopy. *J. Control. Release,* **2000**, *65*(3), 359-366. http://dx.doi.org/10.1016/S0168-3659(99)00213-8 PMID: 10699294

[43] Mai, B.; Gao, Y.; Li, M.; Wang, X.; Zhang, K.; Liu, Q.; Xu, C.; Wang, P. Photodynamic antimicrobial chemotherapy for *Staphylococcus aureus* and multidrug-resistant bacterial burn infection in vitro and in vivo. *Int. J. Nanomedicine,* **2017**, *12*, 5915-5931. http://dx.doi.org/10.2147/IJN.S138185 PMID: 28860757